Nano Research

ISSN 1998-0124 CN 11-5974/O4
https://doi.org/10.1007/s12274-022-4830-4

Research Article

The mechanism of dentine hypersensitivity: Stimuli-induced directional cation transport through dentinal tubules

Nuo Chen[1,§], Jingjing Deng[1,§], Shengjie Jiang[1,§], Xiang-Yu Kong[3,§], Teng Zhou[4,§], Kai Zhao[1], Zuohui Xiao[1], Huimin Zheng[1], Weipeng Chen[3], Congcong Zhu[3,5], Xinyu Liu[1,2], Liping Wen[3,5], Yan Wei[1] (✉), Xuliang Deng[1] (✉), and Lei Jiang[3,5]

[1] *Beijing Laboratory of Biomedical Materials, Department of Geriatric Dentistry, Peking University School and Hospital of Stomatology, Beijing 100081, China*
[2] *Central Laboratory, Peking University School and Hospital of Stomatology, Beijing 100081, China*
[3] *CAS Key Laboratory of Bio-inspired Materials and Interfacial Science, Technical Institute of Physics and Chemistry, Chinese Academy of Sciences, Beijing 100190, China*
[4] *Mechanical and Electrical Engineering College, Hainan University, Hainan 570228, China*
[5] *School of Future Technology University of Chinese Academy of Sciences, Beijing 100049, China*
[§] *Nuo Chen, Jingjing Deng, Shengjie Jiang, Xiang-Yu Kong, and Teng Zhou contributed equally to this work.*

Received: 15 July 2022 / **Revised:** 27 July 2022 / **Accepted:** 27 July 2022

ABSTRACT

Dentine hypersensitivity is an annoying worldwide disease, yet its mechanism remains unclear. The long-used hydrodynamic theory, a stimuli-induced fluid-flow process, describes the pain processes. However, no experimental evidence supports the statements. Here, we demonstrate that stimuli-induced directional cation transport, rather than fluid-flow, through dentinal tubules actually leads to dentine hypersensitivity. The *in vitro*/*in vivo* electro-chemical and electro-neurophysiological approaches reveal the cation current through the nanoconfined negatively charged dentinal tubules coming from external stimuli (pressure, pH, and temperature) on dentin surface and further triggering the nerve impulses causing the dentine hypersensitivity. Furthermore, the cationic-hydrogels blocked dentinal tubules could significantly reduce the stimuli-triggered nerve action potentials and the anion-hydrogels counterpart enhances those, supporting the cation-flow transducing dentine hypersensitivity. Therefore, the inspired ion-blocking desensitizing therapies have achieved remarkable pain relief in clinical applications. The proposed mechanism would enrich the basic knowledge of dentistry and further foster breakthrough initiatives in hypersensitivity mitigation and cure.

KEYWORDS

dentine hypersensitivity, cation transport, dentinal tubules, Ionic-current-rectification

1 Introduction

Dentine hypersensitivity with the manifestation of tiny external stimuli causing the abrupt sharp pain greatly afflicts almost half population in the world [1–6]. The most widely accepted hydrodynamic theory postulates that rapid fluid-flows within tubules transduce external stimuli to nerve terminals [7–11]. This theory proposed in 1900 [12] was supported by observing the stimuli-induced fluid-flow [13–16] and ever since then it has been used in dentistry textbook till today. However, no experimental evidence indicates that such fluid-flow could trigger appropriate neural excitation to lead to dentine hypersensitivity. Moreover, the reduction of fluid-flow has unreliable effect on pain relief in clinical practice [11, 17, 18], which also questions the long-used hydrodynamic theory. Until today, the mechanisms of dentine hypersensitivity remain unclear [19–21]. Along with the development of neuroscience, it has been well established that the essence of pain is actually a sensory process of nervous signal transmission [22–25]. With electro-chemical [26–28] and electro-neurophysiological approaches [29, 30], the ionic functional basis of plenty of crucial somato-sensations has been unveiled, including taste [31, 32], vision [33], smell [34], audition [35], and tactility [36, 37]. As a kind of somato-sensations, dentine hypersensitivity probably belonged to the ionic transportation mediated neural excitation. Follow this clue, we carry out *in vitro*/*in vivo* electro-chemical and electro-neurophysiological experiments to test our idea. The results demonstrate that stimuli applied on dentin surface could be well converted to cationic currents through dentinal tubules, and in turn elicit nerve impulses. The nanoconfined and negatively charged dentinal tubules could control the cation transportation with remarkable ionic-current-rectification properties. As a proof-of-concept, our built fluid-flow blocking model confirms that the stimuli-induced cation flow excites the action potential resulting in aching, which could be the mechanism of dentine hypersensitivity.

2 Experimental

2.1 Animal model

All animal experiments were performed following the guidelines established by Animal Care and Use Committee of Peking

Address correspondence to Yan Wei, kqweiyan@bjmu.edu.cn; Xuliang Deng, kqdengxuliang@bjmu.edu.cn

University (approval number: LA2019321 and SC2021-06-005). For electro-neurophysiological experiments, eighteen-to-twenty-month-old miniature pigs (Chinese Guangxi Bama Miniature pig) were randomly assigned to minimize any potential bias. Miniature pigs were sedated with a cocktail of 4 mg/kg tiletamine hydrochloride and 4 mg/kg zolazepam hydrochloride injected intramuscularly, intubated and mechanically ventilated with positive pressure. Inhalatory anaesthesia was maintained by a mixture of 1%–2% isoflurane dissolved in 40% air and 60% oxygen. Electrocardiogram, heart rate, and arterial pressure were constantly monitored. To construct dentine hypersensitive models, we removed the enamel layer of mandibular molars and made tooth cavity with volume of about 553 mm^3 on the occlusal plane.

2.2 Characterization of dentinal tubules

The sectional optical images of hypersensitive teeth were captured using a single-lens reflex camera（6D2, Canon, Japan). The microstructure of dentinal tubules was examined using a field emission scanning electron microscopy (SEM) (7500F, JEOL) operating at 30 kV, transmission electron microscopy (TEM) (H300, Hitachi) operating at 80 kV, and high angle annular dark field-scanning TEM (HAADF-STEM) (F200X, FEI Talos) operating at 200 kV. To avoid severe deformation of cellular components caused by dehydration, we used a critical point drying technique to prepare the SEM specimens. Dentin sections were cut about 60–80 nm with a diamond knife to prepare the TEM sample. For immunostaining, teeth were decalcified with ethylene diamine tetraacetic acid (EDTA) decalcification solution for 2 weeks and embedded in paraffin. To observe the distribution of glycosaminoglycans, the embedded dentin tissues were sectioned at 5 μm and stained with periodic acid-schiff stain. Images were acquired by light microscopy (CX21, Olympus). To observe the distribution of collagen and fibronectin, the slices were incubated with primary antibody of collagen-1 (Abclonal, A16020, 1:200) and fibronectin (Abcam, ab6328, 1:200) overnight at 4 °C. Then, the slices were stained with secondary antibodies (Abcam, ab150077 and ab150116, 1:200) for 1 h at ambient temperature. The images were captured using a laser confocal microscopy Leica SP8. The surface potential of dentinal tubules was detected by Kelvin probe force microscopy (KPFM) with dimension icon probe tips. Teeth were broken up by forceps in liquid nitrogen and stored in phosphate solution. Scanning capacitance microscopy-Pt/Ir coated tips (SCM-PIT) probe and "Peak Force KPFM-AM" mode were used at the lift height of 100 nm (scanning range 10 μm and scanning rate 1 Hz). To visualize the surface charges in dentinal tubules, ion staining experiments were made by exposing dentin samples to negatively charged rhodamine 6G (Sigma-Aldich, 252433) or positively charged sulfonated rhodamines (Acmec, S13320) staining solution respectively. To observe the permeation of fluorescent dyes passed through dentinal tubules, Ca^{2+} cations and Cl^- anions labelled with fluorescent dyes were put in the tooth cavity respectively. After external stimuli were applied on dentin surface, the solutions in pulp chamber were taken out and observed using a laser confocal microscopy Leica SP8.

2.3 Electrochemical tests

To explore the ion transport behavior of dentinal tubules, Keithley 6487 semiconductor picoammeter (Keithley Instruments, Cleveland, OH) was set on mandibular molars. One Ag/AgCl electrode was placed in tooth cavity filled with a series of KCl solution concentration (10^{-5}, 10^{-4}, 10^{-3}, 10^{-2}, 10^{-1}, 1, and 3 M), and the other Ag/AgCl electrode was inserted into the pulp chamber with body fluid. The ionic current was measured under the voltage of −0.05 to 0.05 V for 10 times. To investigate ionic currents through dentinal tubules in response to various stimuli, we applied pressures (100, 200, 300, and 400 mmHg), pH (5, 5.5, 6, 6.5, 7.5, 8, and 9), and temperature (5, 13, 21, 29, 45, 53, 61, and 69 °C) stimuli respectively on the dentin surface. The stimuli-induced ionic current under the voltage of 0 V was measured for 10 times.

2.4 Electro-neurophysiological tests

To record the stimuli triggered nerve-trunk action potentials, the Ag electrodes of BL-420N signal acquisition system were set on the separated mandibular nerve trunk. Pressure (100 and 400 mmHg), pH (5 and 9), and temperature stimuli (5 and 55 °C) were applied on the dentin surface respectively. To compare the efficiency of ionic mechanism and hydrodynamic theory in triggering neural excitation, the stimuli-corresponding electric currents (Table S1 in the Electronic Supplementary Material (ESM)) and stimuli-corresponding fluid flow (Table S2 in the ESM) were applied on the pulp nerves directly.

2.5 Evaluation of the desensitizing efficacy of cationic hydrogel in clinical trial

Outpatients in Peking University Hospital of Stomatology with dentine hypersensitivity were deemed eligible for this clinical trial after an informed consent. 20 patients having at least 1 hypersensitive tooth with facial-visual analogue scale (F-VAS) of > 3 after air blast stimulation were qualified for participating in the study. The participants were subjected to tactile and air blast stimuli for assessment. The pain feeling was recorded by a F-VAS ranging from 0 to 10 before and after treatment with cationic hydrogel.

2.6 Observation of voltage-gated Na^+ on pulp nerves

Frozen pulp taken from human was embedded in opti-mum cutting temperature compound (OCT) medium (Solarbio, YZ-4583-1EA), and sections of 5 μm were thawed on glass slide. The slices were immersed and fixed in 4% paraformaldehyde for 20 min, washed with phosphate buffered saline (PBS). The samples were incubated overnight with the high molecular weight neurofilament protein neurofilament-H (ABclonal, A19084), Nav1.7 (Proteintech, 20257-1-AP), Nav1.8 (Invitrogen, PA5-77732), and Nav1.9 (Invitrogen, PA5-77733) polyclonal primary antibodies, respectively. The samples were then stained with secondary antibodies (Abcam, ab150077 and ab150116) for 1 h at ambient temperature. The images were captured using a laser confocal microscopy Leica SP8.

2.7 Numerical simulation of ion transportation through the simplified model of dentinal tubules

In this mathematical model, the width of the inside dentin tubule was $W_{ct} = 10^{-6}$ m and the width of the outside dentin tubule was $W_{cd} = 1.5 \times 10^{-6}$ m. The width of the inside cell protrusion was $W_{rt} = 5 \times 10^{-7}$ m and the width of the end of cell protrusion was $W_{rd} = 1.49 \times 10^{-6}$ m. The length of the cell protrusion was $L_r = 0.001$ m and the length of the dentin tubule was $L_c = 0.003$ m. For the purpose of demonstrating the double electrical layer as well as considering the computational cost, the channel from the root up to 400 nm was considered. To ensure that ion current rectification (ICR) phenomenon was obvious in the figure as the current difference was weak, the results were computed by intercepting 800 nm channels from the bottom. The whole model was completely filled with NaCl solution and the primary concentration was 150 mmol/L. The pH of the solution at the inlet was adjusted by adding HCl or NaOH. The density of the negative surface charge on the wall was set as −0.00718 C/m^2.

The initial temperature was $T_0 = 298.15$ K and the diffusion

coefficients of the four ions at this temperature were $D_{Na0} = 1.334 \times 10^{-9}$ m^2/s, $D_{H0} = 9.311 \times 10^{-9}$ m^2/s, $D_{OH} = 5.273 \times 10^{-9}$ m^2/s, and $D_{ClO} = 2.032 \times 10^{-9}$ m^2/s, respectively.

The ionic mass transportation in the electrolyte solution is regarded as Poisson–Nernst–Planck (PNP) equation

$$-\varepsilon_0 \varepsilon_f \nabla^2 \varnothing = \sum_{i=1}^{n} F z_i c_i \quad (1)$$

$$\frac{\partial c_i}{\partial t} + \nabla \cdot N_i = 0 \quad (2)$$

where ε_0 (8.85×10^{-12} F/m) and ε_f are the absolute permittivity of a vacuum and the relative permittivity, respectively, φ is the electrical potential, F is Faraday constant, z_i is the valence of the ith ionic species, c_i is the ionic concentration of the ith ionic species, and n is the total number of ionic species in the electrolyte solution.

The ionic flux within NaCl electrolyte solution arising from convection, diffusion, and electromigration is given by

$$N_i = uc_i - D\nabla c_i - Z_i \frac{D_i}{RT} F c_i \nabla c_i \nabla \varnothing, i = 1 \text{ and } 2 \quad (3)$$

where uc_i is convection term, $D\nabla c_i$ is the diffusion term, $Z_i \frac{D_i}{RT} F c_i \nabla c_i \nabla \varnothing$ is the electromigration term, u is the fluid velocity, D_i is the diffusivity of the ith ionic species, R is the universal gas constant, and T is the absolute temperature of the electrolyte solution.

The flow field in the electrolyte solution is regarded as Stokes equation system as the Reynolds number is low

$$-\nabla p + \mu \nabla 2u - \nabla \varphi \sum_{i=1}^{n} F z_i c_i = 0 \quad (4)$$

$$\nabla \cdot u = 0 \quad (5)$$

where, p is the pressure in liquid.

The boundary conditions for the fluid motion were given as follows: On the walls of the two ends and the surface of the nanochannel, the velocity satisfied the no slip condition. There was no ion flux in the normal direction of the wall. The bulk force in the flow field was the electric field force. The model performed under no pressure difference between the outlet and inlet. The initial flow velocity at the inlet was zero. The total grid number of the model was 49,500, the maximum unit size was 1.35×10^{-10} m, and the minimum was 1.56×10^{-12} m.

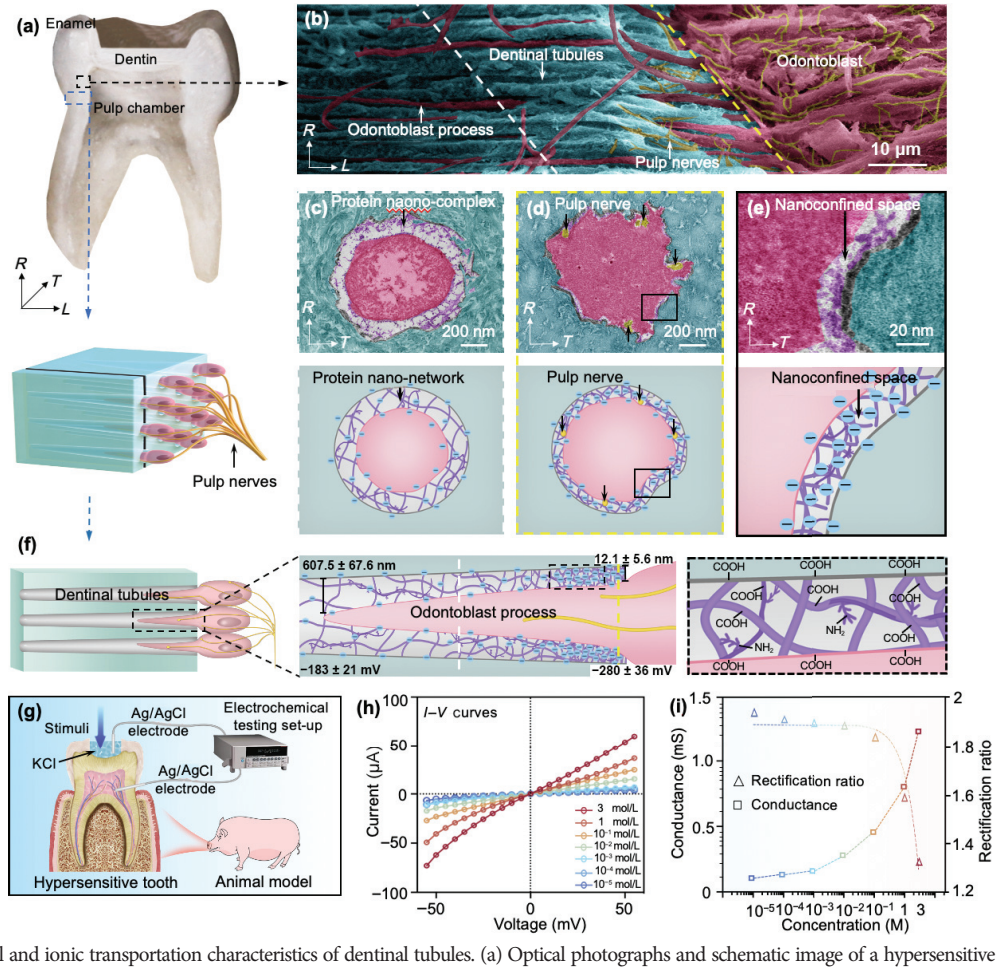

Figure 1 Structural and ionic transportation characteristics of dentinal tubules. (a) Optical photographs and schematic image of a hypersensitive tooth with sectional slice perpendicular to the mid-coronal cervical plane, displaying that dentin as a bulk of tooth serves as the environment-pulp bridge. (b) Pseudocoloured SEM image of the inner third of dentin, clearly showing that parallel-aligned dentinal tubules are penetrated by ondontoblast-process and pulp nerves. (c) and (d) Pseudocoloured cross-sectional view and the corresponding schematic images in the RT plane under TEM at white and yellow line in (b), revealing the existence of protein nano-network in the space confined between tubular wall and odontoblast process. (e) Enlarged TEM image and corresponding schematic image taken from black zone in (g) show the nanoscale width of the confined space. (f) Schematic illustration of the properties of dentinal tubules step by step amplification, showing that dentinal tubules as outside-in junction across whole width of dentin have nanoconfined and negatively charged spaces due to the penetration of pulp cells and the containment of protein complex. (g) Schematic illustration of the *in vivo* functional characterization of a dentine hypersensitivity model using an electrochemical testing system. Ag/AgCl electrode is placed in cavity filled with KCl solution outside of dentin, and the other Ag/AgCl electrode is inserted into the pulp chamber with body fluid. (h) Representative non-linear *I*–*V* curves under a series of KCl solution concentrations at pH 7, revealing an asymmetric ion transport behavior of dentinal tubules. (i) Conductance and rectification ratio of dentinal tubules as a function of KCl solution concentration at pH 7, showing typical surface charge-governed ion transport.

3 Results and discussion

3.1 Structural and ionic transportation characteristics of dentinal tubules

To explore the ionic functional basis of dentine hypersensitivity, we investigate the structural and ionic transportation characteristics of dentinal tubules. Figure 1(a) shows the sectional optical image of a hypersensitive tooth. Once the covered enamel is broken, dentin connects dental pulp with external environment directly. As shown in Fig. 1(b), dentin layer is traversed by parallel-aligned dentinal tubules (Fig. S1 in the ESM) with distribution density of about 20,000 tubules/mm^2 [38, 39]; the inner third of dentinal tubule is penetrated by ondontoblast-process and pulp nerves, forming a confined space between tubular wall and cellular components (Fig. S2 in the ESM). The inner structure of the dentinal tubules is revealed by examining the cross-sections perpendicular to their long axis at different positions, indicating an asymmetric confined space being filled with protein nano-network (Figs. 1(c)–1(e) and Fig. S3 in the ESM). Figure 1(f) illustrates the structure evolution from outer end of the dentinal tubules to the inner pulp chamber. With the containment of pulp cells and protein complex, dentinal tubules hold nanoconfined and negatively charged spaces with decreased widths (607.5 ± 67.6 to 12.1 ± 5.6 nm) (Figs. S4 and S5 in the ESM, and Video ESM1) but increased electrical potentials (−183 ± 21 to −280 ± 36 mV) (Figs. S6 and S7 in the ESM) from the enamel side to the pulp-chamber side. Then, an electrochemical testing system is set on hypersensitive molar teeth model *in vivo* (Fig. 1(g)), in which the enamel is removed. The ion transport behaviors between the external environment and the nerves in pulp chamber are recorded by using a pair of Ag/AgCl electrodes. One electrode is placed in the tooth cavity with different concentration KCl solutions, and the other one is plugged into the pulp chamber. The *I*–*V* curves indicate an asymmetric ion transport behavior (Fig. 1(h)), and the conductance at low concentration shows typical surface charge-governed ion transport (Fig. 1(i)). Thus, nanoconfined and negatively charged dentinal tubules not only bridge the outer environment and the pulp but also govern the ion transport between them.

3.2 Stimuli-induced ion currents through dentinal tubules

Aiming to reveal whether the noxious stimuli in dentine hypersensitivity can be transformed through the ionic mechanism, we characterize the ion transportation behaviors of dentinal tubules in response to various pressure, pH, or temperature, respectively, applied on hypersensitive molar teeth model *in vitro* (Fig. 2(a)). The formed nanoconfined negatively charged spaces are simplified as sloping conical channels for latter theoretical simulation (Fig. 2(b)). Compared with the tooth with intact enamel, the ionic currents keep almost linearly increasing along with the increased pressure in the hypersensitive molar teeth model (Fig. 2(c)). Also, the ionic currents in response to acid are higher than those responding to alkali with the same pH deviation from pH 7 (Fig. 2(d)). For the temperature stimuli, the ionic currents under 0 or 5 °C are significantly higher than that under 55 °C, whereas the current intensities in response to coldness are similar to those in response to heat with the same temperature deviation from 37 °C (Fig. 2(e) and Fig. S8 in the ESM). These

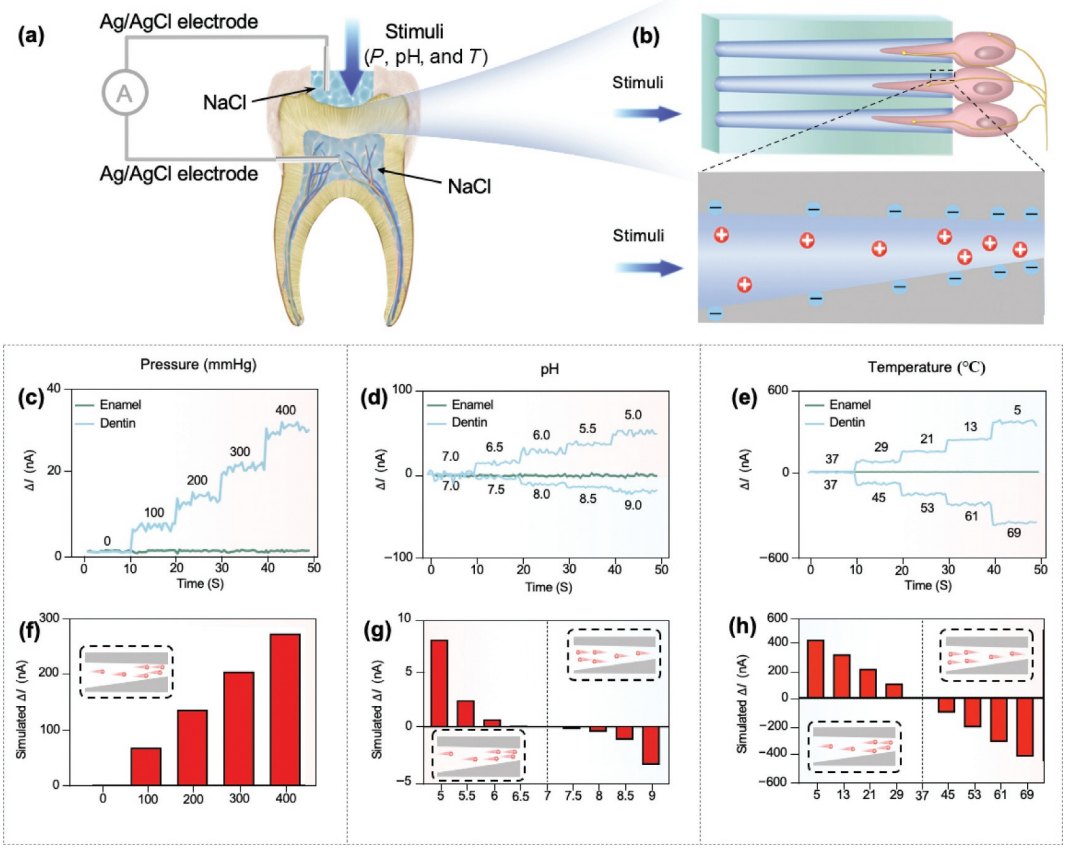

Figure 2 Stimuli-induced ion currents through dentinal tubules. (a) Schematic illustration of the ion currents measurement through dentinal tubules in response to various stimuli applied on dentin surface of extracted tooth with perfusion-fixation. (b) Schematic illustration of theoretical simulating the stimuli induced ion mass transportation through the simplified model of the nanoconfined negatively charged dentinal tubules with PNP equations. (c)–(e) Stimuli-induced ionic currents in response to pressure, pH, and temperature, which are consistent with clinical manifestation of dentine hypersensitivity. (f)–(h) The dose-effect relationship between stimuli and ion currents achieved by theoretical calculation is similar to the experimental results, indicating that the simplified model is representative for dentinal tubules. The schematic images showing that dentinal tubules benefit unique cation transport in numerical simulations.

results are consistent with clinical manifestation of dentine hypersensitivity. Similar dose-effect relationships among pressure, pH, temperature stimuli, and ion currents are also achieved in theoretical calculation using PNP equations (Figs. 2(f)–2(h)), confirming the validation of the proposed model (Fig. S9 in the ESM). Furthermore, numerical simulations demonstrate that the opposite preferential directions of ion currents in response to acid versus alkali and coldness versus heat are resulted from the opposite directions of cation transportation (schematic images in Figs. 2(f)–2(h) and Fig. S10 in the ESM), which is also supported by the experimental results (Fig. S11 in the ESM). The dose-effect relationship between stimuli and ion currents can be ascribed to that varied pressure, pH, or temperature stimuli could trigger proportional ion flow velocity (Fig. S12(a) in the ESM), concentration gradients (Fig. S12(b) in the ESM), or diffusion potential (Fig. S12(c) in the ESM) to directional cation transport, respectively. Based on the experimental and theoretical results, the external stimuli applied on dentin surface could be well converted into unique cation currents through the cation permselective dentinal tubules for signal transmission.

3.3 Stimuli-induced ion currents through dentinal tubules leads dentine hypersensitivity

Following the generated cation current, we further explore the critical role of cation currents in eliciting nerve impulse for the generation of pain sensation in dentine hypersensitivity. Thus, we simultaneously detect the stimuli-induced ion current through dentinal tubules with electrochemical system and stimuli-triggered nerve-trunk action potential with electro-neurophysiological functional system *in vivo* (Fig. 3(a)). Immunofluorescence staining (Fig. S13 in the ESM) shows that the voltage-gated Nav1.7,

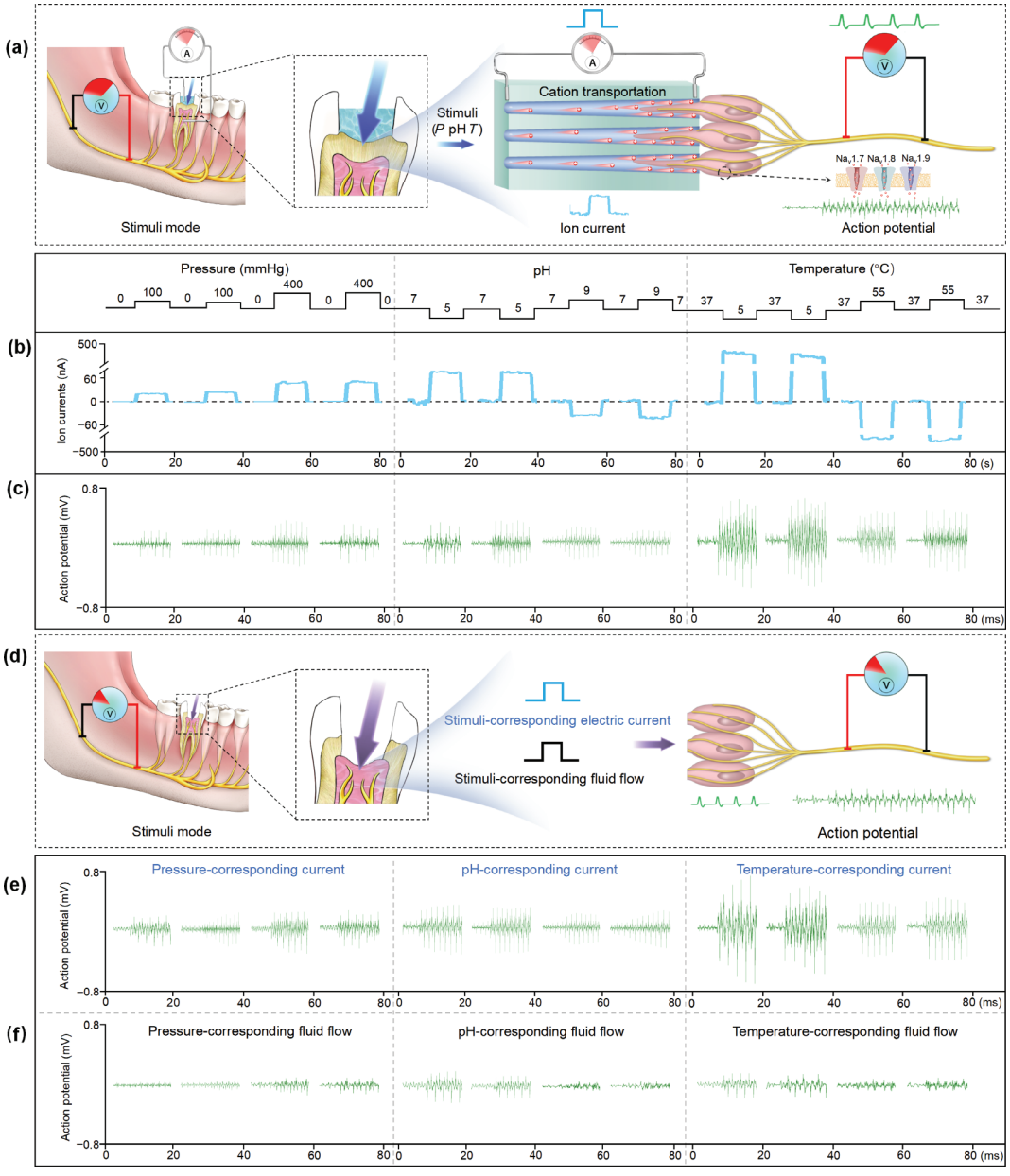

Figure 3 Stimuli-induced ion currents through dentinal tubules lead dentine hypersensitivity. (a) Schematic illustration of the stimuli-induced ion currents through dentinal tubules and the nerve-trunk action potentials as function of various stimuli applied on dentin surface. (b) and (c) The magnitudes of the stimuli-induced ion currents are proportion to the intensity of the stimuli-triggered action potentials, confirming that the ionic currents across the dentinal tubules could elicit neural excitation. (d) Schematic illustration of comparing the efficiency of ionic mechanism and classical hydrodynamic theory in triggering neural excitation for hypersensitive pain sensation. The stimuli-corresponding electric currents or stimuli-corresponding fluid-flow are directly applied on pulp nerves. (e) Action potentials as function of stimuli-corresponding electric currents in ionic mechanism, showing almost the same efficiency to stimuli applied on dentin surface. (f) Action potentials as function of stimuli-corresponding fluid flow in hydrodynamic theory, merely about two orders of magnitude lower than the counterpart evoked by stimuli applied on dentin surface.

Nav1.8, and Nav1.9 channels are highly expressed on pulp nerves, which are critical for the initiation and propagation of pain sensation [40–42]. After applying the pressure, pH, or temperature on dentin surface, respectively, the magnitude of the action potential is proportionate to the current intensity regardless of the current direction (Figs. 3(b) and 3(c)), giving out the explanations of why dentin is unable to distinguish sour from sweet, or hot from icy. Thereafter, we verified our proposed mechanism by directly applying the stimuli-corresponding electric currents in the ionic mechanism or stimuli-corresponding fluid flow in the hydrodynamic theory on pulp nerves (Fig. 3(d)). The efficiency in triggering neural excitation of ionic mechanism and hydrodynamic theory is compared in detail. Impressively, the amplitudes of the resulted nerve action potentials from applying stimuli-corresponding electric currents on pulp nerves and applying stimuli on dentin surface are almost the same (Fig. 3(e)). Meanwhile, the amplitudes of the triggered nerve action potentials from applying stimuli-corresponding fluid flow on pulp nerves are about two orders lower than the counterpart triggered by stimuli applied on dentin surface (Fig. 3(f)). Thus, the stimuli-induced cation currents rather than fluid-flow through dentinal tubules actually dominate dentine hypersensitivity.

3.4 Manipulating dentine hypersensitivity by regulating cation transportation through dentinal tubules

Based on our proposed ionic mechanism of dentine hypersensitivity, we further manipulate the cation transportation through dentinal tubules by plugging their outer part with cationic-hydrogel (CH) or anionic-hydrogel (AH) to explore the potential clinic applications (Fig. 4(a)). Firstly, both CH and AH could significantly decrease the velocities of fluid-flow (Video ESM2). Also, the CH blocking (CHB) effect could well reduce the ionic conductance of dentinal tubules by hindering the cation entering the hydrogel network, whereas the AH blocking (AHB) effect enhances the ionic conductance (Fig. 4(b) and Fig. S14 in the ESM). Consequently, the intensities of stimuli-induced ion

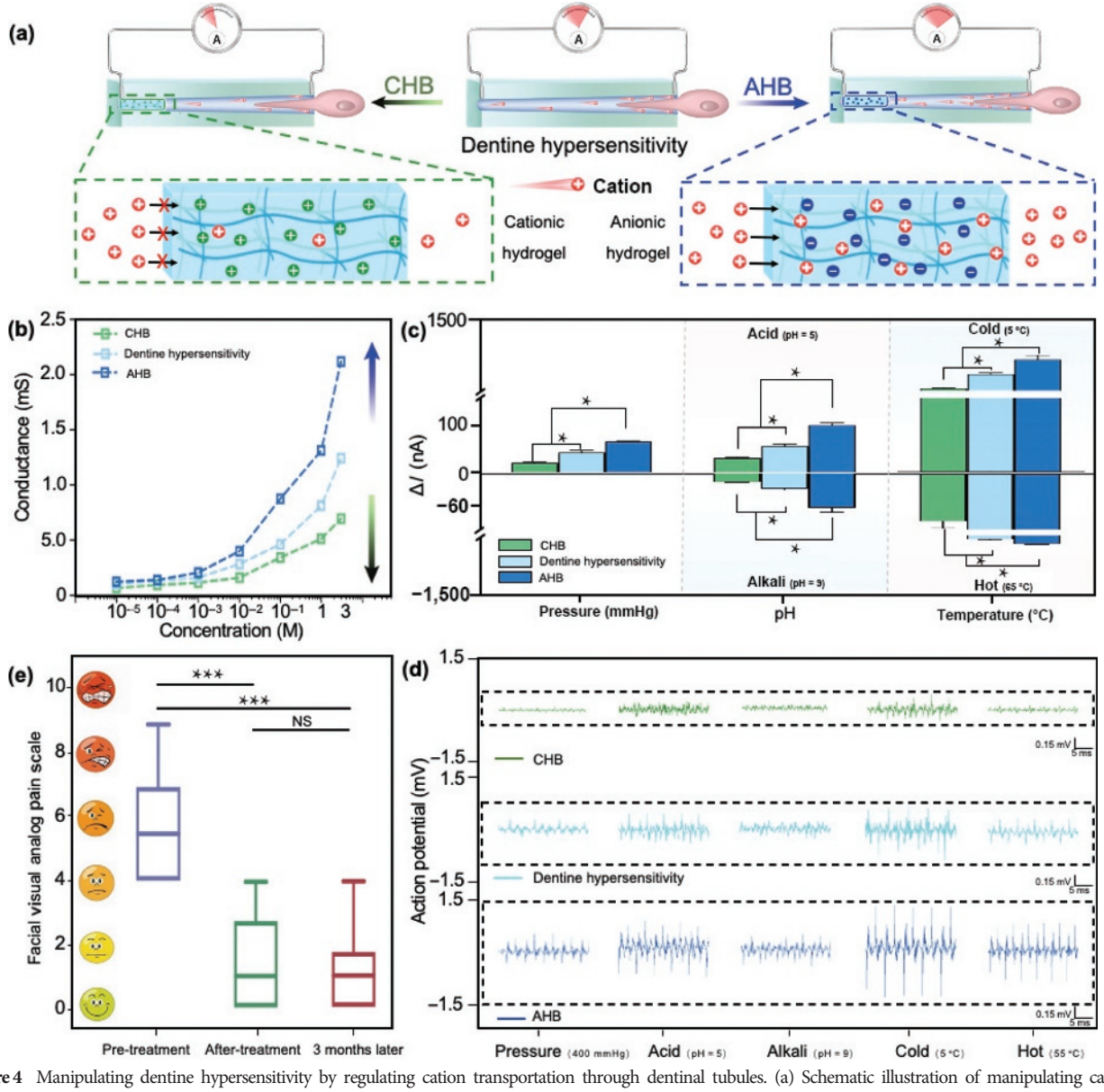

Figure 4 Manipulating dentine hypersensitivity by regulating cation transportation through dentinal tubules. (a) Schematic illustration of manipulating cationic transportation through dentinal tubules by plugging the outer space with CH or AH. (b) Conductance versus KCl solution concentration for dentinal tubules, showing that CH inhibits electric conduction while AH promotes that. (c) Stimuli-induced ion currents through dentinal tubules, displaying that CH decreases the current intensities while the AH increases those. (d) Stimuli-triggered nerve-trunk action potentials. The magnitudes of action potentials are significantly reduced by CH but enhanced by AH, indicating the validities of these hydrogels in manipulating neural excitation for hypersensitive pain sensation. (e) The assessment of pain intensity in twenty patients with dentine hypersensitivity before and after application of CH demonstrates that the ion-blocking significantly relives the pain.

currents through dentinal tubules are reduced by CHB but enhanced by AHB (Fig. 4(c) and Fig. S15 in the ESM). Correspondingly, the magnitudes of nerve action potentials (Fig. 4(d)) in response to pressure, pH, and temperature stimuli are significantly decreased after CHB but increased after AHB, respectively. Based on these results, we develop desensitizing therapies by using CHB in dental clinical application (Fig. S16 in the ESM). The pain feeling of twenty patients with complaint of dentine hypersensitivity is recorded on a F-VAS ranging from 0 to 10. The clinic survey demonstrates that CHB significantly relieves the pain of patients (Fig. 4(e)). Taken together, the positive correlation between the cationic-conductance of dentinal tubules and the stimuli-triggered nerve impulses corroborates the vital role of ion-flow in transducing dentine hypersensitivity and inspires effective ion-based desensitizing therapies for clinical applications.

4 Conclusions

In conclusion, we demonstrate that the directional cation transport through the dentinal tubules is actually the mechanism of dentinal hypersensitivity. The experimental and theoretical results show the ICR characteristics and cation permselectivity of dentinal tubules. Also, the *in vitro*/*in vivo* electro-chemical and electro-neurophysiological tests indicate that the external stimuli applied on dentin surface are well converted to cation currents through dentinal tubules, which downstream excite pulp nerves appropriately to dominate dentine hypersensitivity. Furthermore, the bidirectional manipulated nerve impulses in models with dentinal tubules blocked by cationic- or anionic- hydrogels challenge the classical fluid-flow explanation and validate the critical role of ion-flow. In this regard, we present a desensitizing therapy by using cationic-hydrogel-blocking, which has successfully relieved the pain in clinic application. The ionic mechanism of dentine hypersensitivity revealed here may contribute to the theoretical understanding of the preferential ionic functional basis of somato-sensations and the practical design of novel clinical technology in hypersensitivity mitigation or cure.

Acknowledgements

We thank the National Key R&D Program of China (No. 2020YFA0710401), the National Natural Science Foundation of China (Nos. 82225012, 81922019, 82071161, 81991505, 22122207, 21988102, and 52075138), the Young Elite Scientist Sponsorship Program by CAST (No. 2020QNRC001), and the Beijing Nova Program (No. 211100002121013).

Electronic Supplementary Material: Supplementary material (further details of SEM images, TEM images, KPFM topography maps, immunofluorescence images, electrochemical test, and theoretical calculation) is available in the online version of this article at https://doi.org/10.1007/s12274-022-4830-4.

References

[1] Walters, P. A. Dentinal hypersensitivity: A review. *J. Contemp. Dent. Pract.* **2005**, *6*, 107–117.
[2] Irwin, C. R.; McCusker, P. Prevalence of dentine hypersensitivity in a general dental population. *J. Ir. Dent Assoc.* **1997**, *43*, 7–9.
[3] Bahşi, E.; Dalli, M.; Uzgur, R.; Turkal, M.; Hamidi, M. M.; Colak, H. An analysis of the aetiology, prevalence and clinical features of dentine hypersensitivity in a general dental population. *Eur. Rev. Med. Pharmacol. Sci.* **2012**, *16*, 1107–1116.
[4] Rees, J. S.; Addy, M. A cross-sectional study of dentine hypersensitivity. *J. Clin. Periodontol.* **2002**, *29*, 997–1003.
[5] Dababneh, R. H.; Khouri, A. T.; Addy, M. Dentine hypersensitivity—An enigma? A review of terminology, mechanisms, aetiology and management. *Br. Dent. J.* **1999**, *187*, 606–611.
[6] Bamise, C. T.; Esan, T. A. Mechanisms and treatment approaches of dentine hypersensitivity: A literature review. *Oral. Health Prev. Dent.* **2011**, *9*, 353–367.
[7] West, N. X.; Lussi, A.; Seong, J.; Hellwig, E. Dentin hypersensitivity: Pain mechanisms and aetiology of exposed cervical dentin. *Clin. Oral Investig.* **2013**, *17*, 9–19.
[8] Lindén, L.; Brännström, M. Fluid movements in dentine and pulp. An *in vitro* study of flow produced by chemical solutions on exposed dentine. *Odontol. Revy* **1967**, *18*, 227–236.
[9] Brännström, M. Dentin sensitivity and aspiration of odontoblasts. *J. Am. Dent. Assoc.* **1963**, *66*, 366–370.
[10] Brännström, M.; Aström, A. The hydrodynamics of the dentine; its possible relationship to dentinal pain. *Int. Dent. J.* **1972**, *22*, 219–227.
[11] Mantzourani, M.; Sharma, D. Dentine sensitivity: Past, present and future. *J. Dent.* **2013**, *41*, S3–S17.
[12] Cunha-Cruz, J.; Stout, J. R.; Heaton, L. J.; Heaton, J. C.; For Northwest PRECEDENT. Dentin hypersensitivity and oxalates: A systematic review. *J. Dent. Res.* **2011**, *90*, 304–310.
[13] Addy, M.; Dowell, P. Dentine hypersensitivity - a review. *J. Clin. Periodontol.* **1983**, *10*, 351–363.
[14] Närhi, M.; Kontturi-Närhi, V.; Hirvonen, T.; Ngassapa, D. Neurophysiological mechanisms of dentin hypersensitivity. *Proc. Finn. Dent. Soc.* **1992**, *88*, 15–22.
[15] Gysi, A. An attempt to explain the sensitiveness of dentin. *Br. J. Dent. Sci.* **1900**, *43*, 865–868.
[16] Brännström, M. A hydrodynamic mechanism in the transmission of pain producing stimuli through the dentine. In *Sensory Mechanism in Dentine*. Anderson, D. J. , Ed.; Pergamon Press: Oxford, 1963; pp 73–79.
[17] Brännström, M. The elicitation of pain in human dentine and pulp by chemical stimuli. *Arch. Oral Biol.* **1962**, *7*, 59–62.
[18] Brännström, M. The surface of sensitive dentine. An experimental study using replication. *Odontol. Revy* **1965**, *16*, 293–299.
[19] Brännström, M.; Lindén, L. A.; Aström, A. The hydrodynamics of the dental tubule and of pulp fluid. A discussion of its significance in relation to dentinal sensitivity. *Caries. Res.* **1967**, *1*, 310–317.
[20] Liu, X. X.; Tenenbaum, H. C.; Wilder, R. S.; Quock, R.; Hewlett, E. R.; Ren, Y. F. Pathogenesis, diagnosis and management of dentin hypersensitivity: An evidence-based overview for dental practitioners. *BMC Oral Health* **2020**, *20*, 220.
[21] Linsuwanont, P.; Versluis, A.; Palamara, J. E.; Messer, H. H. Thermal stimulation causes tooth deformation: A possible alternative to the hydrodynamic theory? *Arch. Oral Biol.* **2008**, *53*, 261–272.
[22] Yam, M. F.; Loh, Y. C.; Tan, C. S.; Adam, S. K.; Manan, N. A.; Basir, R. General pathways of pain sensation and the major neurotransmitters involved in pain regulation. *Int. J. Mol. Sci.* **2018**, *19*, 2164.
[23] Dubin, A. E.; Patapoutian, A. Nociceptors: The sensors of the pain pathway. *J. Clin. Investig.* **2010**, *120*, 3760–3772.
[24] Basbaum, A. I.; Bautista, D. M.; Scherrer, G.; Julius, D. Cellular and molecular mechanisms of pain. *Cell* **2009**, *139*, 267–284.
[25] Iwata, K.; Sessle, B. J. The evolution of neuroscience as a research field relevant to dentistry. *J. Dent. Res.* **2019**, *98*, 1407–1417.
[26] Zhao, X. L.; Li, L.; Xie, W. Y.; Qian, Y. C.; Chen, W. P.; Niu, B.; Chen, J. J.; Kong, X. Y.; Jiang, L.; Wen, L. P. pH-regulated thermo-driven nanofluidics for nanoconfined mass transport and energy conversion. *Nanoscale Adv.* **2020**, *2*, 4070–4076.
[27] Xiao, K.; Wan, C. J.; Jiang, L.; Chen, X. D.; Antonietti, M. Bioinspired ionic sensory systems: The successor of electronics. *Adv. Mater.* **2020**, *32*, 2000218.
[28] Xin, W. W.; Xiao, H. Y.; Kong, X. Y.; Chen, J. J.; Yang, L. S.; Niu, B.; Qian, Y. C.; Teng, Y. F.; Jiang, L.; Wen, L. P. Biomimetic nacre-like silk-crosslinked membranes for osmotic energy harvesting. *ACS Nano* **2020**, *14*, 9701–9710.
[29] Yarar, E.; Kuruoglu, E.; Kocabıcak, E.; Altun, A.; Genc, E.; Ozyurek, H.; Kefeli, M.; Marangoz, A. H.; Aydın, K.; Cokluk, C. Electrophysiological and histopathological effects of mesenchymal

stem cells in treatment of experimental rat model of sciatic nerve injury. *Int. J. Clin. Exp. Med.* **2015**, *8*, 8776–8784.
[30] Han, D.; Lu, J. Z.; Xu, L.; Xu, J. G. Comparison of two electrophysiological methods for the assessment of progress in a rat model of nerve repair. *Int. J. Clin. Exp. Med.* **2015**, *8*, 2392–2398.
[31] Murakami, M.; Kijima, H. Transduction ion channels directly gated by sugars on the insect taste cell. *J. Gen. Physiol.* **2000**, *115*, 455–466.
[32] Pérez, C. A.; Margolskee, R. F.; Kinnamon, S. C.; Ogura, T. Making sense with TRP channels: Store-operated calcium entry and the ion channel Trpm5 in taste receptor cells. *Cell Calcium.* **2003**, *33*, 541–549.
[33] Weckström, M.; Laughlin, S. B. Visual ecology and voltage-gated ion channels in insect photoreceptors. *Trends Neurosci.* **1995**, *18*, 17–21.
[34] Brooks, J.; Teng, S. Y.; Wen, J. X.; Nith, R.; Nishida, J.; Lopes, P. Stereo-smell via electrical trigeminal stimulation. In *Proceedings of the 2021 CHI Conference on Human Factors in Computing Systems*, Yokohama, Japan, 2021, pp 1–13.
[35] Dumont, R. A.; Gillespie, P. G. Ion channels: Hearing aid. *Nature* **2003**, *424*, 28–29.
[36] Wu, X. D.; Ahmed, M.; Khan, Y.; Payne, M. E.; Zhu, J.; Lu, C. H.; Evans, J. W.; Arians, A. C. A potentiometric mechanotransduction mechanism for novel electronic skins. *Sci. Adv.* **2020**, *6*, eaba1062.
[37] Chou, H. H.; Nguyen, A.; Chortos, A.; To, J. W. F.; Lu, C. E.; Mei, J. G.; Kurosawa, T.; Bae, W. G.; Tok, J. B. H.; Bao, Z. N. A chameleon-inspired stretchable electronic skin with interactive colour changing controlled by tactile sensing. *Nat. Commun.* **2015**, *6*, 8011.
[38] Schilke, R.; Lisson, J. A.; Bauß, O.; Geurtsen, W. Comparison of the number and diameter of dentinal tubules in human and bovine dentine by scanning electron microscopic investigation. *Arch. Oral Biol.* **2000**, *45*, 355–361.
[39] Giudice, G. L.; Cutroneo, G.; Centofanti, A.; Artemisia, A.; Bramanti, E.; Militi, A.; Rizzo, G.; Favaloro, A.; Irrera, A.; Lo Giudice, R. Dentin morphology of root canal surface: A quantitative evaluation based on a scanning electronic microscopy study. *BioMed. Res. Int.* **2015**, *2015*, 164065.
[40] Hameed, S. Nav1.7 and Nav1.8: Role in the pathophysiology of pain. *Mol. Pain* **2019**, *15*, 1744806919858801.
[41] Zhou, X.; Ma, T. B.; Yang, L. Y.; Peng, S. J.; Li, L. L.; Wang, Z. Q.; Xiao, Z.; Zhang, Q. F.; Wang, L.; Huang, Y. Z. et al. Spider venom-derived peptide induces hyperalgesia in $Na_v1.7$ knockout mice by activating $Na_v1.9$ channels. *Nat. Commun.* **2020**, *11*, 2293.
[42] Yang, F.; Anderson, M.; He, S. Q.; Stephens, K.; Zheng, Y.; Chen, Z. Y.; Raja, S. N.; Aplin, F.; Guan, Y.; Fridman, G. Differential expression of voltage-gated sodium channels in afferent neurons renders selective neural block by ionic direct current. *Sci. Adv.* **2018**, *4*, eaaq1438.